

Review

Recent Developments of Solar Cells from PbS Colloidal Quantum Dots

Tomasz Blachowicz ¹  and Andrea Ehrmann ^{2,*} 

¹ Institute of Physics—Center for Science and Education, Silesian University of Technology, 44-100 Gliwice, Poland; tomasz.blachowicz@polsl.pl

² Faculty of Engineering Sciences and Mathematics, Bielefeld University of Applied Sciences, 33619 Bielefeld, Germany

* Correspondence: andrea.ehrmann@fh-bielefeld.de

Received: 15 February 2020; Accepted: 26 February 2020; Published: 3 March 2020



Abstract: PbS (lead sulfide) colloidal quantum dots consist of crystallites with diameters in the nanometer range with organic molecules on their surfaces, partly with additional metal complexes as ligands. These surface molecules are responsible for solubility and prevent aggregation, but the interface between semiconductor quantum dots and ligands also influences the electronic structure. PbS quantum dots are especially interesting for optoelectronic applications and spectroscopic techniques, including photoluminescence, photodiodes and solar cells. Here we concentrate on the latter, giving an overview of the optical properties of solar cells prepared with PbS colloidal quantum dots, produced by different methods and combined with diverse other materials, to reach high efficiencies and fill factors.

Keywords: colloidal PbS quantum dots; quantum dot solar cells; semiconductor; heterojunction; ligand; open-circuit voltage; short-circuit current; power conversion efficiency; fill factor

1. Introduction

Usually, material properties are defined by the atomic or molecular composition of a material tested at the macro scale. This rule no longer holds when structures become very small, in the range of nanometers, where scaling effects lead to significantly different optical [1–3], chemical [4–6], magnetic [7–9] or other properties of nanoparticles or quantum dots. An interesting method to combine the bottom-up assembly of devices from nanoparticles with the mechanical flexibility of the device is now accessible, with the use of relatively simple chemical procedures based on colloidal semiconductor quantum dots [10]. A general reason for semiconducting quantum dots research and development is that they are universal technologically tunable systems, with adjustable energy levels for lighting and sensing applications.

The core of colloidal semiconductor quantum dots often consists of nanocrystals from some hundred to a thousand atoms of II-VI, III-V or IV-VI semiconductors [11]. On their surface, they bear organic molecules or metal complexes as ligands, as visible in Figure 1 [12].

These ligands build the surface layer between the semiconductor quantum dot and the outside, in this way both influencing and being influenced by an inner and an outer interface. The inorganic/organic surface between quantum dots and ligands thus impacts the electronic structure of the quantum dot [13], as well as interactions with neighboring quantum dots [14].

A highly interesting material to produce such quantum dots is PbS. This IV-VI semiconductor typically has a sodium chloride crystal structure [15] and a temperature-dependent direct band gap between approx. 0.29 eV and 0.45 eV, making it useful for detecting infrared and visible light [16]. Besides macroscopic crystals and epitaxial thin films, PbS is often prepared in the form of

nanocrystallites or quantum dots by diverse methods, from chemical routes [17] to electrodeposition [18] and microorganism-based synthesis [19]. One of the main areas of research and development in which PbS nanocrystallites—typically as colloidal PbS quantum dots—are used is photovoltaic applications. Similar to PbSe, PbS has high photosensitivity in the near-infrared spectrum [20], and allows for the tuning of the optical band gap to a broad range of around 0.7–2.1 eV [21,22], as well as the electronic structure of the quantum dot films and significantly shifting the band edges without large modifications of the band gap [23,24]. PbS colloidal quantum dots also show multiple exciton generation [25,26]. All these properties make PbS quantum dot solar cells belong to the quantum dot solar cells with the highest performance [27–29], and thus making PbS a highly interesting material for solar cells.

This review paper gives an overview of most recent studies on solar cells prepared with PbS colloidal quantum dots, production methods, possible material combinations and the resulting solar cell efficiencies.

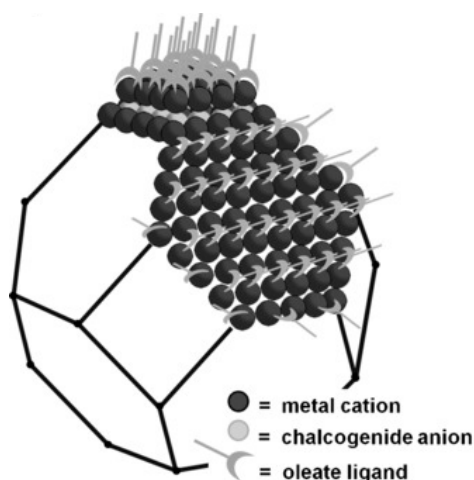


Figure 1. Pb-terminated truncated octahedral PbS quantum dot, depicting Pb cations, S anions and organic ligands. From [12], reprinted with permission. Copyright © Wiley 2016.

2. Solar Cells with PbS Quantum Dots—The Principle Function

With regards to solar cells, the most commercially important technology is based on silicon. There are, however, other technologies, such as those based on perovskites [30], which typically use an active layer from a perovskite material, i.e., a material with the crystal structure ABX_3 , with A denoting a monovalent cation, B a metal cation and X a halide anion [31]. This active layer is usually embedded between two electrodes, one of which has to be transparent to allow photons to reach the active layer, a hole transport layer on the one side and a hole-blocking layer on the opposite side, in this way defining the orientation of the current flow.

Organic solar cells, also named polymer solar cells, also embed the active parts between two electrodes. Usually, the hole transport layer is coated on the anode and the electron transport layer on the cathode. The active layer between them contains electron donors and acceptors [32].

Finally, dye-sensitized solar cells (DSSCs) are of growing interest. While the efficiencies reachable by them are still low, especially when using non-toxic and low-cost materials [33–35], they can be expected to be highly useful in large-scale applications where overall efficiency is less important than the cost-benefit ratio [36]. As the aforementioned types of solar cells, DSSCs contain two conductive electrodes surrounding the other layers. Usually, a semiconductor like TiO_2 or ZnO is applied on the top electrode and dyed with a natural dye, or a more efficient—usually toxic—one. A catalyst is applied on the counter electrode, supporting electrons from an external circuit reaching the active layers of the DSSC. Between a dyed semiconductor and catalyst, an electrolyte fills the gap, usually based on iodine/triiodide or similar redox couples [37].

Generally, quantum dot solar cells enable multi-exciton generation, making such solar cells in principle more efficient than common thin-film or crystal-based ones [38–40]. PbS and other quantum dots can be applied in diverse forms of solar cells, as depicted in Figure 2 [41]. In Schottky junction solar cells, a depletion region is formed due to the band bending between a metal and a p-type semiconductor, the latter possibly being formed by colloidal semiconducting quantum dots. In this Schottky barrier, electron extraction from the device is favored, while holes are withdrawn [42]. Typically, such Schottky solar cells and other solar cell types harvesting light by PbS quantum dots absorb especially near-infrared wavelengths [43].

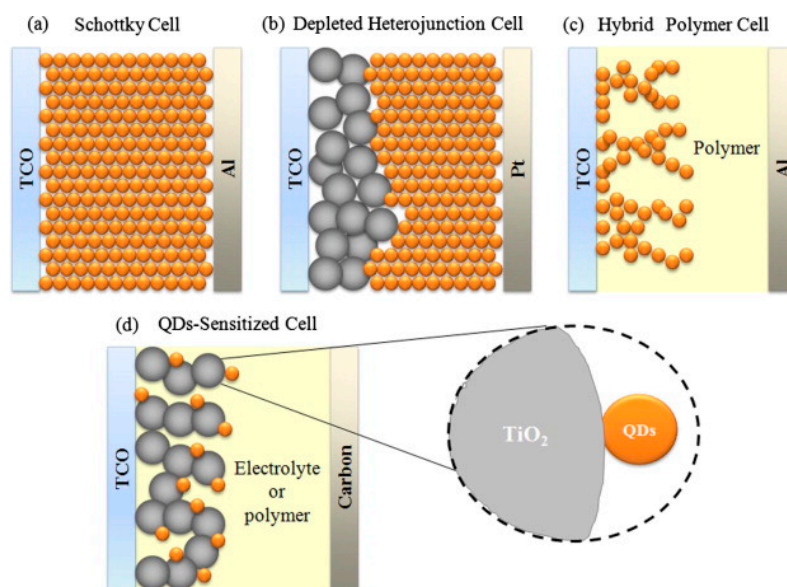


Figure 2. Different quantum dot-based photovoltaic cells. From [41], reprinted with permission. Copyright © Elsevier 2011.

Larger voltages than with Schottky type solar cells can be reached with depleted heterojunction solar cells [41]. With PbS quantum dots, relatively large efficiencies can be reached [44] thanks to electrons flowing towards the TiO_2 layer, while the hole transfer in the opposite direction is prohibited, thus obtaining a high efficiency of carrier separation [45].

Heterojunctions between inorganic and organic parts can also be built with nanocrystals as sensitizers, in combination with a hole transporting polymer [46]. The high expectations due to theoretically high efficiencies could not always be fulfilled, possibly due to reduced contact between both materials [47,48], inefficient charge separation [49] or charge injection at the often used PbS/ TiO_2 interface [50].

As a special heterojunction cell, bulk heterojunction polymer solar cells typically combine electron-donating conjugated polymers with electron-accepting fullerenes. Here, PbS belongs to diverse possible semiconductors which can be added as quantum dots in the original polymer/fullerene composite for light harvesting [51], and sometimes also for electron transport instead of the fullerenes [52].

Finally, quantum dots can be applied as sensitizers in solar cells, similar to the dye molecules in DSSCs. Here, the aforementioned advantage is used so that the band gap can be tailored by geometrical or chemical modifications of the ligands, without changing the material of the quantum dot itself. Like in DSSCs, the excited electron of the quantum dot is inserted into the TiO_2 layer, leading to the oxidation of the quantum dot, and regeneration into the ground state is obtained by the use of an electron from the redox mediator [53]. Like in some other promising approaches, the reachable efficiencies are often lower than expected, e.g., due to surface states of a different nature or back electron transfer [54].

This is why we give here an overview on the most recent results of quantum dot-based solar cells, concentrating on colloidal PbS quantum dots, which can be tailored to start light absorption between 900 nm and 2000 nm, and are thus ideally suited for light harvesting in the near-infrared [55,56].

It should be mentioned that sometimes the boundaries between different types of solar cell are blurred, in which cases the studies are sorted into the sections where they fit best.

3. PbS Quantum Dot Schottky Solar Cells

One recent idea to increase Schottky quantum dot solar cells' (QDSCs) power conversion efficiency is to combine a *p*-type PbS quantum dot layer with an *n*-type metal oxide layer for the front junction [57], or to use inverted Schottky QDSCs with a low-work-function, abstaining from metal oxides [58]. Mai et al. investigated different interfacial electrolytes to fit the electrolyte chemistry to the cell performance [59]. They capped PbS quantum dots (QDs) with oleic acid [58], and passivated them afterwards with Cl⁻. The transparent conductive oxide (TCO) front electrode's work function was lowered by spin-coating the TCO electrode with a few nanometers of polyethylenimine (PEI) or poly [(9,9-bis(3'-(N,N-dimethylamino)propyl)-2,7-fluorene)-alt-2,7-(9,9-dioctylfluorene)] (PFN), respectively. After adding layers of PbS quantum dots, and MoO_x and Au/Ag as a back electrode, the cell was finished. For the different polymer electrolytes used to reduce the work function, the electrical characteristics of the inverted Schottky QDSC changed clearly, as visible in Figure 3. In this way, it was possible to reach an efficiency of 4.5% in an oxide-free QDSC [59].

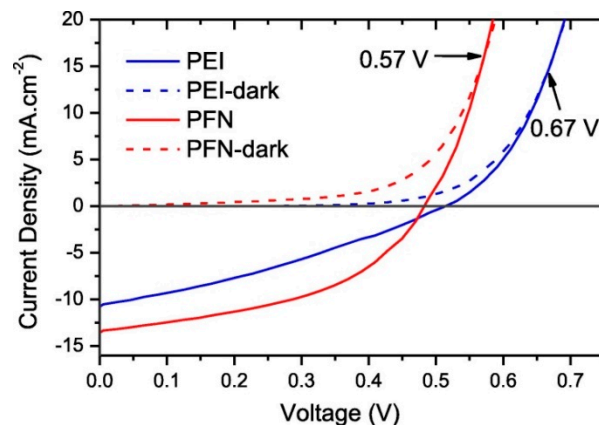


Figure 3. Current density-voltage (J-V) curves of inverted Schottky QDSCs with two different electrolytes. From [59], reprinted with permission. Copyright © Elsevier 2019.

Using ligand-exchanged PbS quantum dots, Fukuda et al. reached a more than twice-as-high photoconversion efficiency [60]. The ligand exchange means that carrier mobility in a quantum dot thin film is increased by a chemical reduction of the ligand length [61]. In this case, soaking the PbS quantum dot thin film in dissolved ethanedithiol (EDT), a typical metal ion ligand, resulted in slightly increased short circuit currents and open circuit voltages, as well as clearly enhanced fill factors [60].

Another way was suggested by Li et al. [62], who used the inorganic-organic hybrid material CH₃NH₃PbI₃ (MAPI) for PbS nanoparticle passivation and investigated the resulting electrical properties of Schottky type solar cells built with these core-shell nanoparticles. It should be mentioned that passivation, in general, is a technology step which reduces surface-related effects and emphasizes the intrinsic bulk-electronic properties. Comparing these core-shell nanoparticles with the original PbS nanoparticles capped with oleic acid/oleylamine, as prepared before the ligand exchange (Figure 4), showed clearly improved electric properties of the corresponding Schottky type solar cell with an approximately five-times higher efficiency than without a ligand exchange. The increased open current voltage was explained by the larger barrier height of the core-shell nanoparticles, in addition to trap state passivation in the quantum dot surface by the MAPI shell, while the improved fill factor and photocurrent were attributed to an enhanced charge transport, based on the lower distance between neighboring quantum dots after the ligand exchange [62].

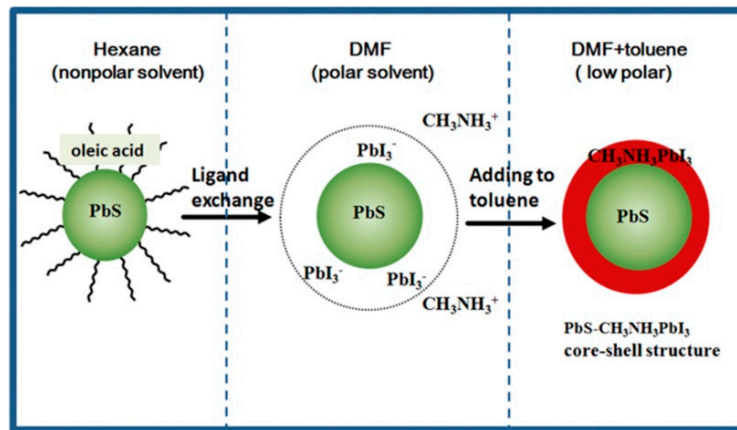


Figure 4. Formation of the PbS-MAPI core-shell nanoparticles by ligand exchange. From [62], reprinted with permission. Copyright © Elsevier 2017.

Similarly, Yang et al. suggested passivating PbS colloidal quantum dots by hybrid ligands prepared from combinations of oleic amine, octyl-phosphine acid and CdCl_2 , and found increased efficiencies in Schottky and p-n junction solar cells, which was attributed to oxidation prevention during device fabrication and shorter chain lengths in the hybrid ligands corresponding to higher hole mobility [63], as also mentioned in [61].

Speirs et al. concentrated on a chemical way to p-dope films of thiol-capped PbS quantum dot, resulting in p-n junction solar cells with an improved short circuit current and fill factor, and thus increased efficiency [64]. While the tetrabutylammonium iodide (TBAI) treatment of PbS resulted in an n-type semiconductor, EDT-capping PbS was used to prepare a p-type semiconductor, as also depicted in Figure 5. p-doping was performed by post-treatment with a sodium hydrosulfide (NaHS) solution, and resulted in an efficiency increase from 7.1% to 7.6%. Investigations of these systems without p-doping showed decreasing electron and hole mobilities with a decreasing temperature, combined with temperature-independent diffusion lengths in EDT-capped PbS and decreasing diffusion length with decreasing temperature in TBAI-capped PbS [65].

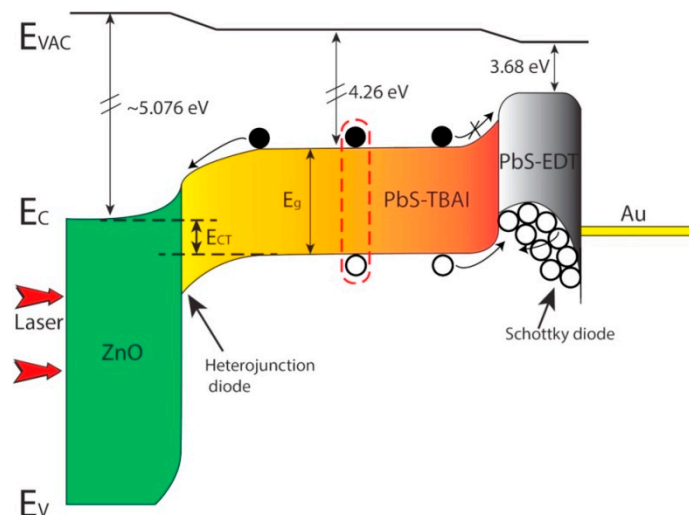


Figure 5. Energy band diagram of a ZnO/PbS-TBAI/PbS-EDT/Au solar cell under illumination, with PbS-EDT working as an electron blocking layer forming a Schottky barrier for holes, thus avoiding their movement to the Au anode. From [66], reprinted with permission. Copyright © Elsevier 2016.

The influence of the hole mobility in such Schottky solar cells with PbS-TBAI and PbS-EDT was simulated by Hu et al., with the corresponding band diagram being depicted in Figure 5 [66]. They found a strongly increasing fill factor and short circuit current for increasing hole mobility until saturation was reached, which was explained by a support of charge carrier extraction to the external anode due to a higher mobility.

Jang et al. concentrated instead on varying the band gap by varying the quantum dot size, in this way enabling building Schottky type solar cells with graded bandgaps. They found higher short circuit current densities combined with lower open circuit voltages in comparison with cells with PbS quantum dots with a uniform bandgap. Under examination, an additional thin electron energy-boosting layer with quantum dots of the highest bandgap could be used to increase both values, in this way improving the overall efficiency [67].

In summary, PbS quantum dots show a high potential for increasing the efficiency of common or inverse Schottky solar cells. The main research focus is placed on the ligands, since ligand exchange or other forms of ligand modification, as well as combinations of PbS quantum dots with different ligands, are promising approaches for further optimization of the Schottky solar cell efficiency.

4. PbS Quantum Dot Sensitized Solar Cells

Light harvesting properties of metal oxides like TiO₂ or ZnO, which are typically applied as semiconducting layers in DSSCs, can be enhanced by decorating them with low bandgap metal sulfides. One of the techniques used for this purpose is the so-called pseudo-successive ionic layer adsorption and reaction (p-SILAR). Ali et al. described in their most recent study how PbS and CdS quantum dots were deposited on TiO₂ nanoparticles, performing a H₂S treatment of the TiO₂ nanoparticles in a rotary reactor. Using rhodamine B degradation as a measure, they showed the positive influence of the H₂S treatment for the p-SILAR process [68].

Ul Hassan et al. improved the p-SILAR technique by a wet chemical modification, as depicted in Figure 6, applying a fluorination treatment of PbS and CdS nanoparticles during centrifugation, resulting in an increased deposition on ZnO nanoparticles and thus a significant increase of the photocurrent density of corresponding solar cells [69].

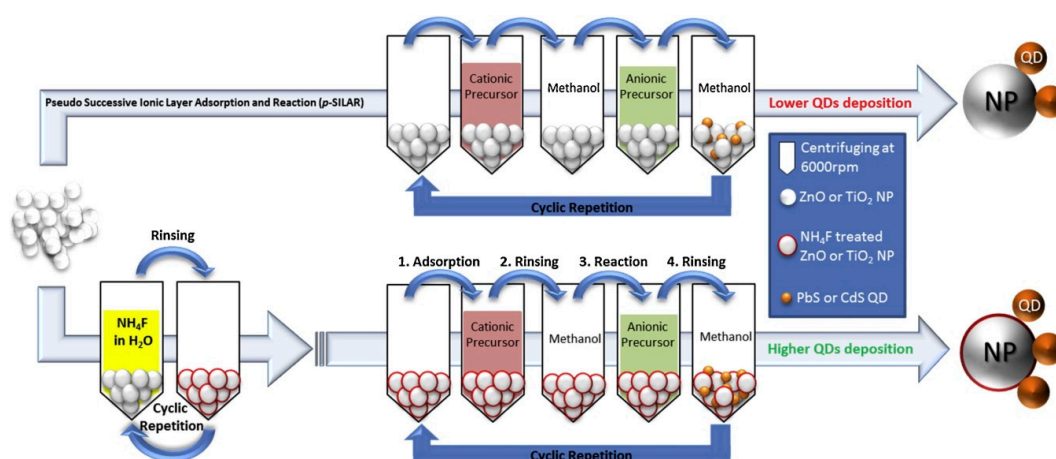


Figure 6. Comparison of the normal (upper row) and the modified p-SILAR process (lower row). From [69], reprinted with permission. Copyright © Elsevier 2016.

With common SILAR, Mao et al. realized a synchronous PbS and CdS quantum dot deposition on TiO₂, in this way avoiding the excessive growth of PbS quantum dots in TiO₂ mesopores and increasing high-density defect passivation on the PbS surface, both leading to a strong increase of solar cell efficiency [70]. Similarly, Kraus et al. reached epitaxial nucleation of PbS quantum dots on a planar TiO₂(100) surface in rutile modification by SILAR [71].

Li et al. applied SnO₂ instead of TiO₂ for quantum dot-sensitized solar cells. They used the aforementioned ligand exchange to reach an improved charge transfer to the sensitized substrate by using short-chain multidentate hydrophilic ligands instead of the common hydrophobic oleic acid ligands, in order to increase electronic coupling to the substrate and at the same time avoid degradation of the PbS-sensitized SnO₂ single crystals in the electrolyte [72].

On the base of ZnO/ZnSe core/shell nanorod arrays decorated with PbS quantum dots by SILAR, Kamruzzaman prepared solar cells with a maximum efficiency of 0.88%, concentrating on the core/shell structure and the nanorod array density rather than optimizing the PbS decoration [73].

Another technique was used by Purcell-Milton et al., who deposited colloidal quantum dots by electrophoretic deposition on TiO₂, increasing the quantum dot loading by optimizing the solvent, as visible in Figure 7. The clear difference in absorption resulted in also suggesting dichloromethane (DCM) as a possible solvent for PbS and other quantum dots [74]. Electrophoretic deposition was also used by Bhardwaj et al. to develop nanocomposite-doped photo-anodes with PbS quantum dots as a sensitizer, showing that the incorporation of TiO₂/Au nanocomposites, the optimization of the quantum dot deposition temperature and the postdeposition annealing of the sensitized photo-anode improved the power conversion efficiency [75].

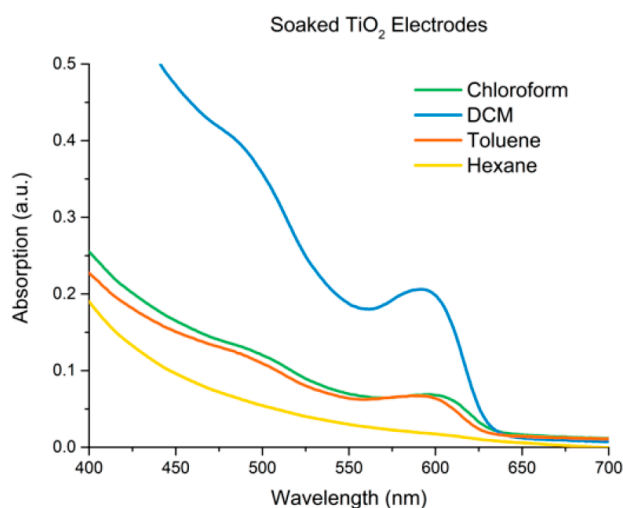


Figure 7. UV/Vis absorption spectra after soaking identical TiO₂ layers in solutions of oleic acid capped CdSe colloidal quantum dots. From [74], originally published under a CC-BY license.

Huang et al. applied PbS colloidal quantum dots as sensitizers on mesoporous TiO₂/CsPbBr₃ perovskite interfaces in solar cells by spin-coating, in this way approximately doubling the power conversion efficiency in comparison with the pristine device [76].

PbS quantum dots were synthesized inside ferritin protein shells by Hansen et al., which protected them from photocorrosion, resulting in quantum dot sensitized solar cells with mesoporous TiO₂, giving efficiencies of around 0.29% when a drop casting method was used [77].

Zhang et al. concentrated on the colloidal PbS quantum dots themselves. They synthesized these quantum dots by air-stable thiourea, stabilized by Cd post-treatment via cation exchange, and found an increased performance of solar cells sensitized with these quantum dots, as compared to devices produced with quantum dots synthesized from common bis(trimethylsilyl) sulfide [78].

Core/shell PbS/CdS quantum dots were applied as photosensitizers on TiO₂ to avoid charge recombination inside the quantum dots and at the quantum dot/TiO₂/electrolyte interfaces, resulting in a significant increase of the power conversion efficiency in comparison with pristine PbS-based quantum dot sensitized solar cells [79]. Park et al., who synthesized PbS quantum dots with embedded CuS, reported even higher efficiencies, which were explained by reduced charge carrier recombination and improved absorptivity [80].

Going beyond the pure function of PbS quantum dots as sensitizers, Wang et al. also used them as carrier transporters. They prepared a heterostructure from PbS quantum dots as absorbers and hole carriers with ZnO nanowires as electron carriers, and showed efficient charge collection along this hybrid structure, which was attributed to band bending in the ZnO dealing as collector, resulting in efficient charge separation and thus large hole transportation distances [81].

Generally, PbS quantum dots show highly interesting sensitizing properties due to the different possibilities to modify their absorption spectra. In addition, they can even be used as charge carriers, allowing for combining two purposes in one material layer.

After this overview on PbS quantum dots as sensitizers in quantum dot sensitized solar cells, the next section will report on further ideas beyond Schottky type and DSSC type solar cells, often combining different physical and chemical properties of PbS quantum dots.

5. PbS Quantum Dot Heterojunction Solar Cells

Plasmonic metal nanoparticles can be used to concentrate incident sunlight by plasmon resonance, in this way increasing the overall absorption of the incident light in a solar cell without increasing the quantum dot film thickness over the carrier diffusion length. Hong et al. used Au and Ag nanoparticles to introduce localized surface plasmon resonance, as well as the scattering of the incident light. By placing the small Au nanoparticles (diameter ~ 10 nm) at the ZnO coated front layer, followed by the PbS active layer and the larger Ag nanoparticles (diameter ~ 50 nm), and then the gold contact back electrode, the latter serves mostly as a far-field scatterer, while the Au nanoparticles enable near-field coupling, in this way increasing the efficiency by approx. 25% [82].

Dastjerdi et al. concentrates on the problem of UV stability of the usual short organic ligands of PbS quantum dots used for solar cells. They used a CdSe/ZnS quantum dot layer to down-shift luminescence on the back of the bulk heterojunction with ZnO nanowires, thus not only increasing the time-stability of the cells, but also their power conversion efficiency, since the UV photons—which were usually thermalized or absorbed in other layers—were now downshifted to visible light, and thus also contributed to power conversion [83].

Xie et al. optimized planar hybrid heterojunction PbS-polymer solar cells by tuning the band gap of the PbS quantum dots between 0.86 eV and 2.1 eV by varying the synthesis temperature (Figure 8), ligand exchange and an optimized production process with a thinner deposited PbS layer. In this way, the performance could be doubled as compared to similar hybrid heterojunction PbS/organic solar cells [84]. Using a variable band-gap structure in quantum dot heterojunction solar cells was also suggested by Ding et al., who used different quantum dot sizes to align the energy levels of the active layer, resulting in a power conversion efficiency increase of more than 20% [85].

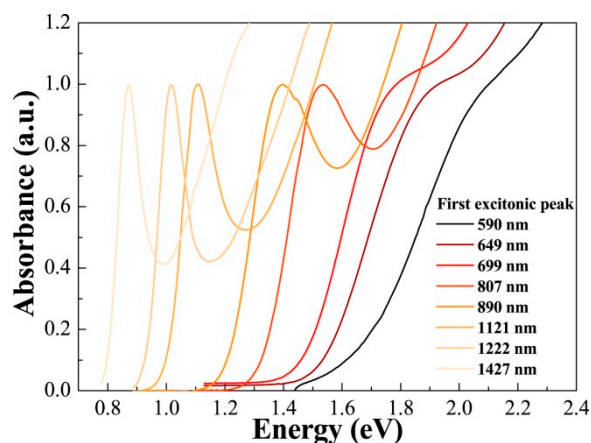


Figure 8. Absorption spectra of PbS quantum dots synthesized at temperatures between 45 °C and 185 °C. From [84], reprinted with permission. Copyright © Elsevier 2019.

The problem of interfacial deficiency between semiconductor and colloidal PbS quantum dots in ordered bulk heterojunction solar cells was investigated by Shi et al. They produced exactly interpenetrating structures of a ZnO nanowire array and PbS colloidal quantum dots by optimizing nanowire growth orientation and using convective assembly to deposit the quantum dots. The resulting dense packing led to a high power conversion efficiency of nearly 10% [86].

Nano-heterojunctions between CdS nanowires surrounded by PbS nanoparticles were developed by Majumder et al. When combining the chemical bath deposition of CdS nanowires with the aforementioned SILAR process for PbS nanoparticle deposition, an increase of the power conversion efficiency by more than one order of magnitude could be reached in corresponding solar cells (Figure 9), which was attributed to the flat band potential, optimized electron lifetime and recombination rate [87].

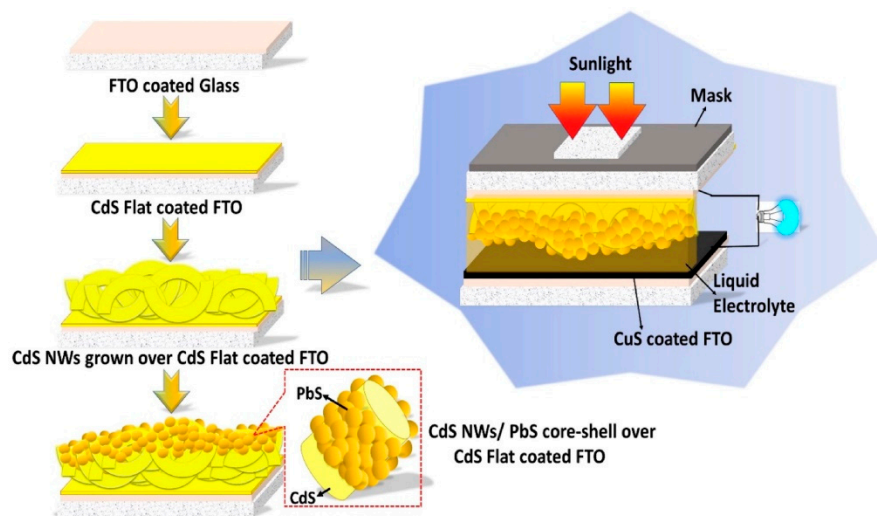


Figure 9. Production process of CdS nanowires on FTO (fluorine-doped tin oxide) glass, SILAR deposition of PbS nanoparticles and final solar cell assembly. From [87], reprinted with permission. Copyright © Elsevier 2019.

Wang et al. optimized the ZnO/PbS heterojunction for a colloidal quantum dot solar cell by passivating defects in the sol-gel ZnO at low temperatures by adding polyethylenimine (PEI) to the precursor solution. In this way, a higher crystallization rate was achieved, the ZnO work function was reduced and the heterojunction interface voltage was increased, which was attributed to improved charge carrier separation in the depletion region. In addition, higher electron mobility was found, while the undesired carrier recombination was suppressed. In this way, the power conversion efficiency could be increased by 25%, as compared to pure ZnO/PbS heterojunction solar cells [88].

Zhao et al. used perovskite/PbS quantum dot heterojunction films to promote hole extraction and decrease carrier recombination in a perovskite solar cell. In comparison with cells without PbS as a hole transporting material, the efficiency could nearly be doubled, and the solar cells showed much higher stability [89].

The interface between TiO₂ and PbS in planar heterojunction solar cells was the focus of a study by Zeng et al. [90]. To suppress surface defects in the electron transport layer between the active PbS layer and the FTO substrate through a TiO₂ layer, thermo-stable hydroxyl radicals were pre-implanted on the TiO₂ nanoparticle surface, in this way creating an electron transport layer, eliminating interband traps by passivating the intrinsic oxygen-deficient defects and matching electron affinity and work function. Thus, undesired interface recombination was suppressed, and power conversion efficiency was strongly increased [90].

Xu et al. improved the interface between the active layer and the anode of a heterojunction quantum dot solar cell by introducing a graphene oxide layer between the PbS active layer and Au anode. By post-annealing, the graphene oxide layer was partly reduced to graphene, worked as a

hole-transport layer and significantly reduced the defects at the PbS/Au interface, finally resulting in an increase in efficiency of 12.9% [91].

Imran et al. prepared bulk heterojunction organic solar cells based on the electron-donating organic semiconductor P3HT-poly(3-hexylthiophene) and the electron accepting fullerene PCBM [6,6]-phenyl-C61-butyric acid methyl ester with various ratios of the inorganic semiconductor PbS. Here, the PbS nanoparticles decreased the series resistance, and thus improved the power conversion efficiency of these solar cells [92].

Since traditional PbS quantum dot solar cell structures require high-temperature fabrication of an inorganic buffer layer, an inverted structure was proposed by some groups [93,94]. Wang et al. built an effective p-n heterojunction in an inverted colloidal quantum dot solar cell by using NiO for the *p*-type layer and PbS colloidal quantum dots with iodide ligands for the *n*-type layer. Due to the large depletion region, a large photocurrent was achieved. At the same time, interface carrier recombination was prohibited by an additional slightly doped *p*-type quantum dot layer with EDT as ligands, which improved the device voltage, leading to strongly enhanced power conversion efficiency [95].

Spin-coated colloidal PbS quantum dot films were ligand-exchanged to methylammonium iodide (MAI) and used in depleted heterojunction solar cells with TiO₂ as a semiconductor, resulting in a more than doubled power conversion efficiency, as compared to common oleic-acid passivated PbS quantum dot films [96]. Chang et al. used ligand exchange to 3-mercaptopropionic acid, thioglycolic acid and 4-mercaptopbenzoic acid to examine the significant impact of ligand structures on the photovoltaic performance of quantum dot heterojunction solar cells [97]. Wang et al. and Zhang et al. used different ligands and quantum dot dimensions to vary the quantum dot energy levels [98,99].

To avoid undesired charge recombination between ZnO nanowires and PbS quantum dots in a depleted bulk heterojunction solar cell, Zang et al. inserted an ultrathin Al₂O₃ layer between these materials, which clearly increased open-circuit voltage, as well as the short-circuit current and thus the power conversion efficiency [100]. Pradhan et al. reduced interfacial recombination between these materials by a nanocrystal buffer layer, mixing ZnO nanocrystals with PbS quantum dots (Figure 10), in this way improving the charge collection efficiency and thus the overall power conversion efficiency [101]. Zhao et al. introduced a CdI₂ treated CdSe quantum dot buffer layer between ZnO nanoparticles and PbS quantum dots in colloidal PbS heterojunction solar cells [102], while Zang et al. used an ultrathin Mg(OH)₂ layer for this purpose [103].

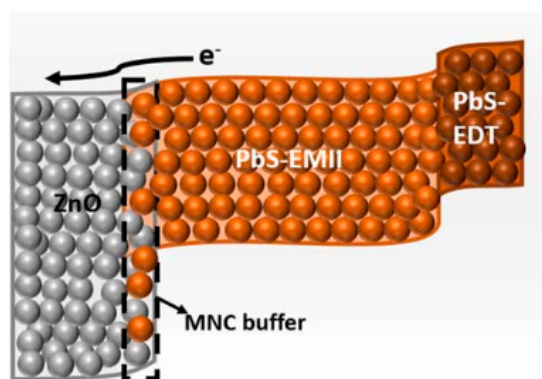


Figure 10. Scheme of energy band alignment of the solar cell with inserted mixed nanocrystal (MNC) layer between ZnO, PbS treated with 1-ethyl-3-methylimidazolium iodide (EMII) as an active layer and PbS-EDT electron blocking layer, in short-circuit condition. Reprinted with permission from [101]. Copyright (2017) American Chemical Society.

Hu et al. examined the influence of CdS thin films used for electron transport in TiO₂/PbS heterojunction colloidal quantum dot solar cells. They used a single-source precursor to prepare solution-processed CdS thin films by spin-coating and annealing, and found increased power conversion

efficiencies compared to cells with CdS layers prepared with chemical bath deposition or RF magnetron sputtering [104].

Another semiconductor, SnO₂, was suggested by Khan et al. to produce colloidal quantum dot heterojunction solar cells. Based on its larger band-gap and higher electron mobility, as compared to the often applied ZnO, as well as adequate band alignment with the PbS quantum dots, light absorption and photocarrier extraction were supported, resulting in high power conversion efficiency [105].

Similarly to [74], Wu et al. found a significant influence of the solvent used to prepare PbS/TiO₂ heterojunction solar cells from different PbS solutions. They reached the highest power conversion efficiency of 7.64% in an n-octane/isooctane hybrid solvent [106].

To summarize, for heterojunction solar cells similar points as for the aforementioned types of solar cells are important, tuning the quantum dot band gap to desired values and increasing the time-stability of the common short ligands on PbS quantum dots. Special difficulties also occur according to the band alignment of semiconductor, the PbS quantum dot layer and possible additional charge transport layers. Nevertheless, PbS quantum dots offer a wide range of possible utilizations in heterojunction solar cells, underlined by the large number of studies published in this research area.

6. Conclusions

As this excerpt of some of the most recent, highly interesting and promising research on PbS quantum dots for solar cells shows, this material offers a broad bandwidth of applications, from light harvesting to electron transport, and correspondingly a large amount of possible solar cell types in which it can be utilized—in particular, the possibility to tailor the semiconductor band gap by changing quantum dot dimensions or ligands makes PbS an interesting material for solar cells with diverse material combinations. On the other hand, controlling quantum dot and ligand properties is necessary to gain sufficient power conversion efficiencies if this material is used in the solar cells of different types.

We hope that our brief review stimulates more research groups working in similar areas to expand their studies towards investigations of this relatively uncomplicated and inexpensive material class, to further increase the possible efficiencies and transfer recent research results into developing industrially suitable processes for the mass market.

Author Contributions: Conceptualization, T.B. and A.E.; visualization, T.B. and A.E.; writing—original draft preparation, A.E. and T.B. All authors have read and agreed to the published version of the manuscript.

Funding: This research received no external funding.

Conflicts of Interest: The authors declare no conflict of interest.

References

1. Storhoff, J.J.; Lazarides, A.A.; Mucic, R.C.; Mirkin, C.A.; Letsinger, R.L.; Schatz, G.C. What controls the optical properties of DNA-linked gold nanoparticle assemblies? *J. Am. Chem. Soc.* **2000**, *122*, 4640–4650. [[CrossRef](#)]
2. Lopez, R.; Feldman, L.C.; Haglund, R.F., Jr. Size-dependent optical properties of VO₂ nanoparticle arrays. *Phys. Rev. Lett.* **2004**, *93*, 177403. [[CrossRef](#)] [[PubMed](#)]
3. Byers, C.P.; Zhang, H.; Swearer, D.F.; Yorulmaz, M.; Hoener, B.S.; Huang, D.; Hoggard, A.; Chang, W.S.; Mulvaney, P.; Ringe, E.; et al. From tunable core-shell nanoparticles to plasmonic drawbridges: Active control of nanoparticle optical properties. *Sci. Adv.* **2015**, *1*, e1500988. [[CrossRef](#)] [[PubMed](#)]
4. Pfeiffer, C.; Rehbock, C.; Hühn, D.; Carillo-Carrion, C.; Jimenez De Aberasturi, D.; Merk, V.M.; Barcikowski, S.; Parak, W.J. Interaction of colloidal nanoparticles with their local environment: The (ionic) nanoenvironment around nanoparticles is different from bulk and determines the physico-chemical properties of the nanoparticles. *J. R. Soc. Interface* **2014**, *11*, 20130931. [[CrossRef](#)]
5. Horie, M.; Fujita, K.; Kato, H.; Endoh, S.; Nishio, K.; Komaba, L.K.; Nakamura, A.; Miyauchi, A.; Kinugasa, S.; Hagihara, Y.; et al. Association of the physical and chemical properties and the cytotoxicity of metal oxide nanoparticles: Metal ion release, adsorption ability and specific surface area. *Metallomics* **2012**, *4*, 350–360. [[CrossRef](#)]

6. Wang, X.; Hanson, J.C.; Liu, G.; Rodriguez, J.A.; Iglesias-Juez, A.; Fernández-García, M. The behavior of mixed-metal oxides: Physical and chemical properties of bulk $Ce_{1-x}Tb_xO_2$ and nanoparticles of $Ce_{1-x}Tb_xO_y$. *J. Chem. Phys.* **2004**, *121*, 5434–5444. [[CrossRef](#)]
7. Sudsom, D.; Juhász Junger, I.; Döpke, C.; Blachowicz, T.; Hahn, L.; Ehrmann, A. Micromagnetic simulation of vortex development in magnetic bi-material bow-tie structures. *Condens. Matter* **2020**, *5*, 5. [[CrossRef](#)]
8. Sturm, S.; Sigleitmeier, M.; Wolf, D.; Vogel, K.; Gratz, M.; Faivre, D.; Lubk, A.; Büchner, B.; Sturm (née Rosseeva), E.V.; Cölfen, H. Magnetic nanoparticle chains in gelatin ferrogels: Bioinspiration from magnetotactic bacteria. *Adv. Funct. Mater.* **2019**, *29*, 1905996. [[CrossRef](#)]
9. Blachowicz, T.; Kosmalska, D.; Döpke, C.; Leiste, H.; Hahn, L.; Ehrmann, A. Varying steps in hysteresis loops of Co square nano-frames. *J. Magn. Magn. Mater.* **2019**, *491*, 165619. [[CrossRef](#)]
10. Kagan, C.R.; Lifshitz, E.; Sargent, E.H.; Talapin, D.V. Building devices from colloidal quantum dots. *Science* **2016**, *353*, aac5523. [[CrossRef](#)]
11. Talapin, D.V.; Lee, J.S.; Kovalenko, M.V.; Shevchenko, E.V. Prospects of colloidal nanocrystals for electronic and optoelectronic applications. *Chem. Rev.* **2010**, *110*, 389–458. [[CrossRef](#)] [[PubMed](#)]
12. Grisorio, R.; Debellis, D.; Suranna, G.P.; Gigli, G.; Giansante, C. The dynamic organic/inorganic interface of colloidal PbS quantum dots. *Angew. Chem. Int. Ed. Engl.* **2016**, *55*, 6628. [[CrossRef](#)] [[PubMed](#)]
13. Giansante, C.; Infante, I.; Fabiano, E.; Grisorio, R.; Suranna, G.P.; Gigli, G. “Darker-than-Black” PbS Quantum Dots: Enhancing Optical Absorption of Colloidal Semiconductor Nanocrystals via Short Conjugated Ligands. *J. Am. Chem. Soc.* **2015**, *137*, 1875–1886. [[CrossRef](#)] [[PubMed](#)]
14. Li, R.; Bian, K.; Hanrath, T.; Bassett, W.A.; Wang, Z. Decoding the Superlattice and Interface Structure of Truncate PbS Nanocrystal-Assembled Supercrystal and Associated Interaction Forces. *J. Am. Chem. Soc.* **2014**, *136*, 12047–12055. [[CrossRef](#)]
15. Kittel, C. *Introduction to Solid State Physics*, 3rd ed.; John Wiley: New York, NY, USA, 1966.
16. Dalven, R. A Review of the semiconductor properties of PbTe, PbSe, PbS and PbO. *Infrared Phys.* **1969**, *9*, 141–184. [[CrossRef](#)]
17. Wang, C.; Zhang, W.X.; Qian, X.F.; Zhang, X.M.; Xie, Y.; Qian, Y.T. A room temperature chemical route to nanocrystalline PbS semiconductor. *Mater. Lett.* **1999**, *40*, 255–258. [[CrossRef](#)]
18. Nanda, K.K.; Sahu, S.N. One-dimensional quantum confinement in electrodeposited PbS nanocrystalline semiconductors. *Adv. Mater.* **2001**, *13*, 280–283. [[CrossRef](#)]
19. Kowshik, M.; Vogel, W.; Urban, J.; Kulkarni, S.K.; Paknikar, K.M. Microbial synthesis of semiconductor PbS nanocrystallites. *Adv. Mater.* **2002**, *14*, 815–818. [[CrossRef](#)]
20. Li, Y.; Zhu, J.; Huang, Y.; Wei, J.; Liu, F.; Shao, Z.; Hu, L.; Chen, S.; Yang, S.; Tang, J.; et al. Efficient inorganic solid solar cell composed of perovskite and PbS quantum dots. *Nanoscale* **2015**, *7*, 9902–9907. [[CrossRef](#)]
21. Gao, J.; Luther, J.M.; Semonin, O.E.; Ellingson, R.J.; Nozik, A.J.; Beard, M.C. Quantum dot size dependent J-V characteristics in heterojunction ZnO/PbS quantum dot solar cells. *Nano Lett.* **2011**, *11*, 1002–1008. [[CrossRef](#)]
22. Talapin, D.V.; Murray, C.B. PbSe Nanocrystal solids for N- and P-channel thin film field-effect Transistors. *Science* **2005**, *310*, 86–89. [[CrossRef](#)] [[PubMed](#)]
23. Yuan, M.J.; Liu, M.X.; Sargent, E.H. Colloidal quantum dot solids for solution-processed solar cells. *Nat. Energy* **2016**, *1*, 16016. [[CrossRef](#)]
24. Brown, P.R.; Kim, D.H.; Lunt, R.R.; Zhao, N.; Bawendi, M.G.; Grossman, J.C.; Bulovic, V. Energy level modification in lead sulfide quantum dot thin films through ligand exchange. *ACS Nano* **2014**, *8*, 5863–5872. [[CrossRef](#)] [[PubMed](#)]
25. Scholes, G.D.; Rumbles, G. Excitons in nanoscale systems. *Nat. Mater.* **2006**, *5*, 683–696. [[CrossRef](#)] [[PubMed](#)]
26. Sambur, J.B.; Novet, T.; Parkinson, B.A. Multiple exciton collection in a sensitized photovoltaic system. *Science* **2010**, *330*, 63–66. [[CrossRef](#)] [[PubMed](#)]
27. Hanna, M.C.; Ellingson, R.J.; Beard, M.; Yu, P.; Micic, O.I.; Nozik, A.J. Quantum dot solar cells: High efficiency through multiple exciton generation. In Proceedings of the 2004 DOE Solar Energy Technologies, Denver, CO, USA, 25–28 October 2004.
28. Zhao, N.; Osedach, T.P.; Chang, L.Y.; Geyer, S.M.; Wanger, D.; Binda, M.T.; Arango, A.C.; Bawendi, M.G.; Bulovic, V. Colloidal PbS quantum dot solar cells with high fill factor. *ACS Nano* **2010**, *4*, 3743–3752. [[CrossRef](#)] [[PubMed](#)]

29. Ip, A.H.; Thon, S.M.; Hoogland, S.; Voznyy, O.; Zhitomirsky, D.; Debnath, R.; Levina, L.; Rollny, L.R.; Carey, G.H.; Fischer, A.; et al. Hybrid passivated colloidal quantum dot solids. *Nat. Nanotechnol.* **2012**, *7*, 577–582. [[CrossRef](#)]
30. Yang, W.S.; Park, B.W.; Jung, E.H.; Jeon, N.J.; Kim, Y.C.; Lee, D.U.; Shin, S.S.; Seo, J.; Kim, E.K.; Noh, J.H.; et al. Iodide management in formamidinium-lead-halide-based perovskite layers for efficient solar cells. *Science* **2017**, *356*, 1376–1379. [[CrossRef](#)]
31. Wang, D.; Wright, M.; Elumalai, N.K.; Uddin, A. Stability of perovskite solar cells. *Sol Energy Mater. Sol. Cells* **2016**, *147*, 255–275. [[CrossRef](#)]
32. Li, Y.; Xu, G.; Cui, C.; Li, Y. Flexible and semitransparent organic solar cells. *Adv. Energy Mater.* **2018**, *8*, 1701791. [[CrossRef](#)]
33. Kohn, S.; Wehlage, D.; Juhász Junger, I.; Ehrmann, A. Electrospinning a dye-sensitized solar cell. *Catalysts* **2019**, *9*, 975. [[CrossRef](#)]
34. Juhász Junger, I.; Udomrungkajornchai, S.; Grimmelsmann, N.; Blachowicz, T.; Ehrmann, A. Effect of caffeine copigmentation of anthocyanin dyes on the DSSC efficiency. *Materials* **2019**, *12*, 2692. [[CrossRef](#)] [[PubMed](#)]
35. Mamun, A.; Trabelsi, M.; Klöcker, M.; Sabantina, L.; Großerhode, C.; Blachowicz, T.; Grötsch, G.; Cornelissen, C.; Streitenberger, A.; Ehrmann, A. Electrospun nanofiber mats with embedded non-sintered TiO₂ for dye-sensitized solar cells (DSSCs). *Fibers* **2019**, *7*, 60. [[CrossRef](#)]
36. Ehrmann, A.; Blachowicz, T. Recent coating materials for textile-based solar cells. *AIMS Mater. Sci.* **2019**, *6*, 234–251. [[CrossRef](#)]
37. Ye, M.; Wen, X.; Wang, M.; Iocozzia, J.; Zhang, N.; Lin, C.; Lin, Z. Recent advances in dye-sensitized solar cells: From photoanodes, sensitizers and electrolytes to counter electrodes. *Mater. Today* **2015**, *18*, 155–162. [[CrossRef](#)]
38. Sikhovatkin, S.; Hinds, S.; Brzozowski, L.; Sargent, E.H. Colloidal quantum-dot photodetectors exploiting multiexciton generation. *Science* **2009**, *324*, 1542–1544. [[CrossRef](#)]
39. Pijpers, J.J.H.; Ulbricht, R.; Tielrooij, K.J.; Oshero, A.; Golan, Y.; Delerue, C.; Allan, G.; Bonn, M. Assessment of carrier-multiplication efficiency in bulk PbSe and PbS. *Nat. Phys.* **2009**, *5*, 811–814. [[CrossRef](#)]
40. Beard, M.C.; Knutsen, K.P.; Yu, P.; Luther, J.M.; Song, Q.; Metzger, W.K.; Ellingson, R.J.; Nozik, A.J. Multiple exciton generation in colloidal silicon nanocrystals. *Nano Lett.* **2007**, *7*, 2506–2512. [[CrossRef](#)]
41. Emin, S.; Singh, S.; Han, L.; Satoh, N.; Islam, A. Colloidal quantum dot solar cells. *Sol. Energy* **2011**, *85*, 1264–1282. [[CrossRef](#)]
42. Clifford, J.P.; Johnston, K.W.; Levina, L.; Sargent, E.H. Schottky barriers to colloidal quantum dot films. *Appl. Phys. Lett.* **2007**, *91*, 253117. [[CrossRef](#)]
43. Tang, J.; Wang, X.; Brzozowski, L.; Barkhouse, A.; Debnath, R.; Levina, L.; Sargent, E.H. Schottky quantum dot solar cells stable in air under solar illumination. *Adv. Mater.* **2010**, *22*, 1398–1402. [[CrossRef](#)]
44. Pattantyus-Abraham, A.G.; Kramer, I.J.; Barkhouse, A.R.; Wang, X.; Konstantatos, G.; Debnath, R.; Levina, L.; Raabe, I.; Nazeeruddin, M.K.; Grätzel, M.; et al. Depleted-heterojunction colloidal quantum dot solar cells. *ACS Nano* **2010**, *4*, 3374–3380. [[CrossRef](#)] [[PubMed](#)]
45. Debnath, R.; Greiner, M.T.; Kramer, J.J.; Füscher, A.; Tang, J.; Barkhouse, D.A.R.; Wang, X.; Levina, L.; Lu, Z.-H.; Sargent, E.H. Depleted-heterojunction colloidal quantum dot photovoltaics employing low-cost electrical contacts. *Appl. Phys. Lett.* **2010**, *97*, 023109. [[CrossRef](#)]
46. Chang, J.A.; Rhee, J.H.; Im, S.H.; Lee, Y.H.; Kim, H.J.; Seok, S.I.; Nazeeruddin, M.K.; Grätzel, M. High-performance nanostructured inorganic–organic heterojunction solar cells. *Nano Lett.* **2010**, *10*, 2609–2612. [[CrossRef](#)] [[PubMed](#)]
47. Nadarajah, A.; Word, R.C.; VanSant, K.; Könenkamp, R. Nanowire-quantum-dot-polymer solar cells. *Phys. Stat. Sol.* **2008**, *245*, 1834–1837. [[CrossRef](#)]
48. Kniprath, R.; Rabe, J.P.; McLeskey, J.T.; Wang, D.; Kirstein, S. Hybrid photovoltaic cells with II–VI quantum dot sensitizers fabricated by layer-by-layer deposition of water-soluble components. *Thin Solid Films* **2009**, *518*, 295–298. [[CrossRef](#)]
49. Plass, R.; Serge, P.; Krüger, J.; Grätzel, M.; Bach, U. Quantum dot sensitization of organic–inorganic hybrid solar cells. *J. Phys. Chem. B* **2002**, *106*, 7578–7580. [[CrossRef](#)]

50. Acharya, K.P.; Hewa-Kaskarage, N.N.; Alabi, T.R.; Nemitz, I.; Khon, E.; Ullrich, B.; Anzenbacher, P.; Zamkov, M. Synthesis of PbS/TiO₂ colloidal heterostructures for photovoltaic applications. *J. Phys. Chem. C* **2010**, *114*, 12496–12504. [[CrossRef](#)]
51. Arenas-Arrocena, M.C.; Mendoza, N.; Cortina-Marrero, H.J.; Nicho, M.E.; Hu, H. Influence of poly(3-octylthiophene) (P3OT) film thickness and preparation method on photovoltaic performance of hybrid ITO/CdS/P3OT/Au solar cells. *Sol. Energy Mater. Sol. Cells* **2010**, *94*, 29–33. [[CrossRef](#)]
52. Dayal, S.; Reese, M.O.; Ferguson, A.J.; Ginley, D.S.; Rumbles, G.; Kopidakis, N. The effect of nanoparticle shape on the photocarrier dynamics and photovoltaic device performance of poly(3-hexylthiophene): CdSe nanoparticle bulk heterojunction solar cells. *Adv. Funct. Mater.* **2010**, *20*, 2629–2635. [[CrossRef](#)]
53. Vogel, R.; Pohl, K.; Weller, H. Sensitization of highly porous, polycrystalline TiO₂ electrodes by quantum sized CdS. *Chem. Phys. Lett.* **1990**, *174*, 241–245. [[CrossRef](#)]
54. Shalom, M.; Dor, S.; Rühle, S.; Grinis, L.; Zaban, A. Core/CdS quantum dot/shell mesoporous solar cells with improved stability and efficiency using an amorphous TiO₂ coating. *J. Phys. Chem. C* **2009**, *113*, 3895–3898. [[CrossRef](#)]
55. Peumans, P.; Yakimov, A.; Forrest, S.R. Small molecular weight organic thin-film photodetectors and solar cells. *J. Appl. Phys.* **2003**, *93*, 3693. [[CrossRef](#)]
56. Maria, A.; Cyr, P.W.; Klem, E.J.D.; Levina, L.; Sargent, E.H. Solution-processed infrared photovoltaic devices with > 10% monochromatic internal quantum efficiency. *Appl. Phys. Lett.* **2005**, *87*, 213112. [[CrossRef](#)]
57. Chuang, C.H.; Brown, P.R.; Bulovic, V.; Bawendi, M.G. Improved performance and stability in quantum dot solar cells through band alignment engineering. *Nat. Mater.* **2014**, *13*, 796–801. [[CrossRef](#)] [[PubMed](#)]
58. Mai, X.-D.; An, H.J.; Song, J.H.; Jang, J.; Kim, S.; Jeong, S. Inverted Schottky quantum dot solar cells with enhanced carrier extraction and air-stability. *J. Mater. Chem. A* **2014**, *2*, 20799–20805. [[CrossRef](#)]
59. Mai, V.-T.; Duong, N.-H.; Mai, X.-D. Boosting the current density in inverted Schottky PbS quantum dot solar cells with conjugated electrolyte. *Mater. Lett.* **2019**, *249*, 37–40. [[CrossRef](#)]
60. Fukuda, T.; Takahashi, A.; Takahira, K.; Wang, H.B.; Kubo, T.; Segawa, H. Limiting factor of performance for solution-phase ligand-exchanged PbS quantum dot solar cell. *Sol. Energy Mater. Solar Cells* **2019**, *195*, 220–227. [[CrossRef](#)]
61. Kagan, C.R.; Murray, C.B. Charge transport in strongly coupled quantum dot solids. *Nat. Nanotechnol.* **2015**, *10*, 1013–1026. [[CrossRef](#)]
62. Li, M.; Yuan, X.; Ruan, H.; Wang, X.; Liu, Y.; Lu, Z.; Hai, J. Synthesis of PbS-CH₃NH₃PbI₃ core-shell nanoparticles with enhanced photoelectric properties. *J. Alloys Compd.* **2017**, *706*, 395–400. [[CrossRef](#)]
63. Yang, Y.; Zhao, B.; Gao, Y.; Liu, H.; Tian, Y.; Qin, D.; Wu, H.; Huang, W.; Hou, L. Novel Hybrid Ligands for Passivating PbS Colloidal Quantum Dots to Enhance the Performance of Solar Cells. *Nanomicro Lett.* **2015**, *7*, 325–331. [[CrossRef](#)] [[PubMed](#)]
64. Speirs, M.J.; Balazs, D.M.; Dirin, D.N.; Kovalenko, M.V.; Loi, M.A. Increased efficiency in pn-junction PbS QD solar cells via NaHS treatment of the p-type layer. *Appl. Phys. Lett.* **2017**, *110*, 103904. [[CrossRef](#)]
65. Speirs, M.J.; Dirin, D.N.; Abdu-Aguye, M.; Balazs, D.M.; Kovalenko, M.V.; Loi, M.A. Temperature dependent behaviour of lead sulfide quantum dot solar cells and films. *Energy Environ. Sci.* **2016**, *9*, 2916. [[CrossRef](#)]
66. Hu, L.; Mandelis, A.; Lan, X.; Melnikov, A.; Hoogland, S.; Sargent, E.H. Imbalanced charge carrier mobility and Schottky junction induced anomalous current-voltage characteristics of excitonic PbS colloidal quantum dot solar cells. *Sol. Energy Mater. Sol. Cells* **2016**, *155*, 155–165. [[CrossRef](#)]
67. Jang, J.; Song, J.H.; Choi, H.; Baik, S.J.; Jeong, S. Photovoltaic light absorber with spatial energy band gradient using PbS quantum dot layers. *Sol. Energy Mater. Sol. Cells* **2015**, *141*, 270–274. [[CrossRef](#)]
68. Ali, I.; Muhyuddin, M.; Mullani, N.; Kim, D.W.; Kim, D.H.; Basit, M.A.; Park, T.J. Modernized H₂S-treatment of TiO₂ nanoparticles: Improving quantum-dot deposition for enhanced photocatalytic performance. *Curr. Appl. Phys.* **2020**, *20*, 384–390. [[CrossRef](#)]
69. Ul Hassan, F.; Ahmed, U.; Muhyuddin, M.; Yasir, M.; Ashiq, M.N.; Basit, M.A. Tactical modification of pseudo-SILAR process for enhanced quantum-dot deposition on TiO₂ and ZnO nanoparticles for solar energy applications. *Mater. Res. Bull.* **2019**, *120*, 110588. [[CrossRef](#)]
70. Mao, X.; Yu, J.; Xu, J.; Zhou, J.; Luo, C.; Wang, L.; Niu, H.; Xu, J.; Zhou, R. Enhanced performance of all solid-state quantum dot-sensitized solar cells via synchronous deposition of PbS and CdS quantum dots. *New J. Chem.* **2020**, *44*, 505–512. [[CrossRef](#)]

71. Kraus, S.; Bonn, M.; Canovas, E. Room-temperature solution-phase epitaxial nucleation of PbS quantum dots on rutile TiO₂ (100). *Nanoscale Adv.* **2020**, *2*, 377–383. [[CrossRef](#)]
72. Li, G.; Yang, Q.; Kubie, L.; Stecher, J.T.; Galazka, Z.; Uecker, R.; Parkinson, B.A. Sensitization of SnO₂ Single Crystals with Multidentate-Ligand-Capped PbS Colloid Quantum Dots to Enhance the Photocurrent Stability. *ChemNanoMat* **2020**. [[CrossRef](#)]
73. Kamruzzan, M. The effect of ZnO/ZnSe core/shell nanorod arrays photoelectrodes on PbS quantum dot sensitized solar cell performance. *Nanoscale Adv.* **2020**, *2*, 286–295. [[CrossRef](#)]
74. Purcell-Milton, F.; Curutchet, A.; Gun'ko, Y. Electrophoretic Deposition of Quantum Dots and Characterisation of Composites. *Materials* **2019**, *12*, 4089. [[CrossRef](#)]
75. Bhardwaj, S.; Pal, A.; Chatterjee, K.; Rana, T.; Bhattacharya, G.; Roy, S.S.; Chowdhury, P.; Sharma, G.D.; Biswas, S. Enhanced efficiency of PbS quantum dot-sensitized solar cells using plasmonic photoanode. *J. Nanoparticle Res.* **2018**, *20*, 198. [[CrossRef](#)]
76. Huang, M.; Lu, Z.; Wen, L.; Zhang, X.; Huang, T.; Meng, Y.; Tang, J.; Zhou, L. Core/shell-structured TiO₂/PbS photoanodes for high-performance CsPbBr₃ perovskite solar cells. *Mater. Lett.* **2019**, *256*, 126619. [[CrossRef](#)]
77. Hansen, K.R.; Peterson, J.R.; Perego, A.; Shelley, M.; Olsen, C.R.; Perez, L.D.; Hogg, H.L.; Watt, R.K.; Colton, J.S. Lead sulfide quantum dots inside ferritin: Synthesis and application to photovoltaics. *Appl. Nanosci.* **2018**, *8*, 1687–1699. [[CrossRef](#)]
78. Zhang, H.; Selopal, G.S.; Zhou, Y.; Tong, X.; Benetti, D.; Jin, L.; Navarro-Pardo, F.; Wang, Z.; Sun, S.H.; Zhao, H.; et al. Controlled synthesis of near-infrared quantum dots for optoelectronic devices. *Nanoscale* **2017**, *9*, 16843–16851. [[CrossRef](#)] [[PubMed](#)]
79. Jiao, S.; Wang, J.; Shen, Q.; Li, Y.; Zhong, X. Surface engineering of PbS quantum dot sensitized solar cells with a conversion efficiency exceeding 7%. *J. Mater. Chem. A* **2016**, *4*, 7214–7221. [[CrossRef](#)]
80. Park, J.P.; Heo, J.H.; Im, S.H.; Kim, S.W. Highly efficient solid-state mesoscopic PbS with embedded CuS quantum dot-sensitized solar cells. *J. Mater. Chem. A* **2016**, *4*, 785–790. [[CrossRef](#)]
81. Wang, H.; Gonzales-Pedro, V.; Kubo, T.; Fabregat-Santiago, F.; Bisquert, J.; Sanehira, Y.; Nakazaki, J.; Segawa, H. Enhanced Carrier Transport Distance in Colloidal PbS Quantum-Dot-Based Solar Cells Using ZnO Nanowires. *J. Phys. Chem. C* **2015**, *119*, 27265–27274. [[CrossRef](#)]
82. Hong, J.; Kim, B.S.; Hou, B.; Cho, Y.; Lee, S.H.; Pak, S.; Morris, S.M.; Sohn, J.I.; Cha, S. Plasmonic Effects of Dual-Metal Nanoparticle Layers for High-Performance Quantum Dot Solar Cells. *Plasmonics* **2020**. [[CrossRef](#)]
83. Dastjerdi, H.T.; Prochowic, D.; Yadav, P.; Tavakoli, M.M. Luminescence down-shifting enables UV-stable and efficient ZnO nanowire-based PbS quantum dot solar cells with J(SC) exceeding 33 mA cm⁻². *Sustain. Energy Fuels* **2019**, *3*, 3128–3134. [[CrossRef](#)]
84. Xie, Q.; Ming, S.; Chen, L.; Wu, Y.; Zhang, W.; Liu, X.; Cao, M.; Wang, H.; Fang, J. Parameters in planar quantum dot-polymer solar cell: Tuned by QD Eg, ligand exchange and fabrication process. *Org. Electron.* **2019**, *69*, 1–6. [[CrossRef](#)]
85. Ding, C.; Zhang, Y.H.; Liu, F.; Nakazawa, N.; Huang, Q.X.; Hayase, S.; Ogomi, Y.; Toyoda, T.; Wang, R.X.; Shen, Q. Recombination Suppression in PbS Quantum Dot Heterojunction Solar Cells by Energy-Level Alignment in the Quantum Dot Active Layers. *ACS Appl. Mater. Interfaces* **2018**, *10*, 26142–26152. [[CrossRef](#)] [[PubMed](#)]
86. Shi, G.; Kaewprajak, A.; Ling, X.; Hayakawa, A.; Zhou, S.; Song, B.; Kang, Y.; Hayashi, T.; Altun, M.E.; Nakaya, M.; et al. Finely Interpenetrating Bulk Heterojunction Structure for Lead Sulfide Colloidal Quantum Dot Solar Cells by Convective Assembly. *ACS Energy Lett.* **2019**, *4*, 960–967. [[CrossRef](#)]
87. Majumder, S.; Mendhe, A.C.; Sankapal, B.R. Nanoheterojunction through PbS nanoparticles anchored CdS nanowires towards solar cell application. *Int. J. Hydrogen Energy* **2019**, *44*, 7095–7107. [[CrossRef](#)]
88. Wang, L.; Jia, Y.; Wang, Y.; Zang, S.; Wei, S.; Li, J.; Zhang, X. Defect Passivation of Low-Temperature Processed ZnO Electron Transport Layer with Polyethylenimine for PbS Quantum Dot Photovoltaics. *ACS Appl. Energy Mater.* **2019**, *2*, 1695–1701. [[CrossRef](#)]
89. Zhao, G.; Cai, Q.; Liu, X.; Li, P.; Zhang, Y.; Shao, G.; Liang, C. PbS QDs as Electron Blocking Layer Toward Efficient and Stable Perovskite Solar Cells. *IEEE J. Photovolt.* **2019**, *9*, 194–199. [[CrossRef](#)]
90. Zeng, T.; Su, X.; Feng, S.; Xie, Y.; Chen, Y.; Shen, Z.; Shi, W. Thermally-stable hydroxyl radicals implanted on TiO₂ electron transport layer for efficient carrier extraction in PbS quantum dot photovoltaics. *Sol. Energy Mater. Sol. Cells* **2018**, *188*, 263–272. [[CrossRef](#)]

91. Xu, J.; Wang, H.; Wang, Y.; Yang, S.; Ni, G.; Zou, B. Efficiency enhancement for solution-processed PbS quantum dots solar cells by inserting graphene oxide as hole-transporting and interface modifying layer. *Org. Electron.* **2018**, *58*, 270–275. [[CrossRef](#)]
92. Imran, M.; Ikram, M.; Anjum, S.; Ali, S.; Huang, Y. Highly Efficient Hybrid Bulk Heterojunction Organic Solar Cells Integrating PbS Nanoparticles. *Nanosci. Nanotechnol. Lett.* **2018**, *10*, 1644–1650. [[CrossRef](#)]
93. Xu, W.Z.; Tan, F.R.; Liu, Q.; Liu, X.S.; Jiang, Q.W.; Wei, L.; Zhang, W.F.; Wang, Z.J.; Qu, S.C.; Wang, Z.G. Efficient PbS QD solar cell with an inverted structure. *Sol. Energy Mater. Sol. Cells* **2017**, *159*, 503–509. [[CrossRef](#)]
94. Luan, W.; Zhang, C.; Luo, L.; Yuan, B.; Jin, L.; Kim, Y.-S. Enhancement of the photoelectric performance in inverted bulk heterojunction solid solar cell with inorganic nanocrystals. *Appl. Energy* **2017**, *185*, 2217–2223. [[CrossRef](#)]
95. Wang, R.L.; Wu, X.; Xu, K.; Zhou, W.; Shang, Y.; Tang, H.; Chen, H.; Ning, Z. Highly Efficient Inverted Structural Quantum Dot Solar Cells. *Adv. Mater.* **2018**, *30*, 1704882. [[CrossRef](#)] [[PubMed](#)]
96. Tavakoli, M.M.; Simchi, A.; Tavakoli, R.; Fan, Z. Organic Halides and Nanocone Plastic Structures Enhance the Energy Conversion Efficiency and Self-Cleaning Ability of Colloidal Quantum Dot Photovoltaic Devices. *J. Phys. Chem. A* **2017**, *121*, 9757–9765. [[CrossRef](#)]
97. Chang, J.; Ogomi, Y.H.; Ding, C.; Zhnang, Y.H.; Toyoda, T.; Hayase, S.; Katayama, K.; Shen, Q. Ligand-dependent exciton dynamics and photovoltaic properties of PbS quantum dot heterojunction solar cells. *Phys. Chem. Chem. Phys.* **2017**, *19*, 6358–6367. [[CrossRef](#)] [[PubMed](#)]
98. Wang, H.; Zhai, G.; Zhang, J.; Yang, Y.Z.; Liu, X.G.; Li, X.; Xu, B.-S. PbS Quantum Dots: Size, Ligand Dependent Energy Level Structures and Their Effects on the Performance of Heterojunction Solar Cells. *J. Inorg. Mater.* **2016**, *31*, 915–922.
99. Zhang, N.; Neo, D.C.J.; Tazawa, Y.; Li, X.; Assender, H.E.; Compton, R.G.; Watt, A.A.R. Narrow Band Gap Lead Sulfide Hole Transport Layers for Quantum Dot Photovoltaics. *ACS Appl. Mater. Interfaces* **2016**, *8*, 21417–21422. [[CrossRef](#)]
100. Zang, S.; Wang, Y.; Li, M.; Su, W.; An, M.; Zhang, X.; Liu, Y. Performance enhancement of ZnO nanowires/PbS quantum dot depleted bulk heterojunction solar cells with an ultrathin Al₂O₃ interlayer. *Chin. Phys. B* **2018**, *27*, 018503. [[CrossRef](#)]
101. Pradhan, S.; Stavrinadis, A.; Gupta, S.; Konstantatos, G. Reducing Interface Recombination through Mixed Nanocrystal Interlayers in PbS Quantum Dot Solar Cells. *ACS Appl. Mater. Interfaces* **2017**, *9*, 27390–27395. [[CrossRef](#)]
102. Zhao, T.; Goodwin, E.D.; Guo, J.; Wang, H.; Diroll, B.T.; Murray, C.B.; Kagan, C.R. Advanced Architecture for Colloidal PbS Quantum Dot Solar Cells Exploiting a CdSe Quantum Dot Buffer Layer. *ACS Nano* **2016**, *10*, 9267–9273. [[CrossRef](#)]
103. Zang, S.; Wang, Y.; Su, W.; Zhu, H.; Li, G.; Zhang, X.; Liu, Y. Increased open-circuit voltage of ZnO nanowire/PbS quantum dot bulk heterojunction solar cells with solution-deposited Mg(OH)₂ interlayer. *Phys. Stat. Sol. Rapid Res. Lett.* **2016**, *10*, 745–748. [[CrossRef](#)]
104. Hu, L.; Patterson, R.J.; Hu, Y.; Chen, W.J.; Zhang, Z.L.; Yuan, L.; Chen, Z.H.; Conibeer, G.J.; Wang, G.; Huang, S. High Performance PbS Colloidal Quantum Dot Solar Cells by Employing Solution-Processed CdS Thin Films from a Single-Source Precursor as the Electron Transport Layer. *Adv. Funct. Mater.* **2017**, *27*, 1703687. [[CrossRef](#)]
105. Khan, J.; Yang, X.; Qiao, K.; Deng, H.; Zhang, J.; Liu, Z.; Ahmad, W.; Zhang, J.H.; Li, D.B.; Liu, H.; et al. Low-temperature-processed SnO₂-Cl for efficient PbS quantum-dot solar cells via defect passivation. *J. Mater. Chem. A* **2017**, *5*, 17240–17247. [[CrossRef](#)]
106. Wu, R.; Yang, Y.; Li, M.; Qin, D.; Zhang, Y.; Hou, L. Solvent Engineering for High-Performance PbS Quantum Dots Solar Cells. *Nanomaterials* **2017**, *7*, 201. [[CrossRef](#)]

